Inorganic Chemistry

pubs.acs.org/IC Communication

Superconductivity Induced by Site-Selective Arsenic Doping in Mo_5Si_3

Bin-Bin Ruan,* Jun-Nan Sun, Meng-Hu Zhou, Qing-Song Yang, Ya-Dong Gu, Gen-Fu Chen, Lei Shan, and Zhi-An Ren*

Cite This: *Inorg. Chem.* 2022, 61, 10267−10271 Read Online

ACCESS | Metrics & More | Article Recommendations | Supporting Information

ABSTRACT: Arsenic doping in silicides has been much less studied compared with phosphorus. In this study, superconductivity is successfully induced by As doping in Mo_5Si_3. The superconducting transition temperature (T_c) reaches 7.7 K, which is higher than those in previously known W_5Si_3-type superconductors. Mo_5Si_2As is a type-II BCS superconductor with upper and lower critical fields of 6.65 T and 22.4 mT, respectively. In addition, As atoms are found to selectively take the 8*h* sites in Mo_5Si_2As. The emergence of superconductivity is possibly due to the shift of Fermi level as a consequence of As doping, as revealed by the specific heat measurements and first-principles calculations. Our work provides not only another example of As doping but also a practical strategy to achieve superconductivity in silicides through Fermi level engineering.

Arsenic doping in elemental silicon has been known for more than half a century.[1] And the kinetics for As diffusion in silicon had been well established.[2,3] However, reports on arsenic doping in silicides are unexpectedly scarce. To the best of our knowledge, there are only 5 examples in bulk materials, namely: $Cr_3Si_{1-x}As_x$,[4] Fe_5SiAs,[5] $ZrSi_{1-x}As_xTe$,[6] and $Zr(Hf)As_{2-x}Si_x$.[7,8]

On the other hand, phosphorus doping had been reported in more than 30 silicides: $CoSi_{0.4}P_{0.6}$,[9] $USi_{0.17}P_{0.83}$,[10] Fe_5SiP,[5] $Nb_5Si_{3-x}P_{0.5+x}$,[11] $Gd_5Si_{4-x}P_x$,[12] and MSi_xP_y (M = Fe, Co, Ru, Rh, Pd, Os, Ir, and Pt, and $x + y \geq 4$),[13,14] to name a few. Compared to the P dopant, the much less studied As doping offers an opportunity to chase for new compounds in this field.

Our group has been working on MoAs-based superconductors, and has discovered a series of quasi-one-dimensional superconductors $A_2Mo_3As_3$ (A = K, Rb, Cs).[15−17] Recently, superconductivity was reported in Re-doped Mo_5Si_3 with a transition temperature (T_c) of 5.8 K, setting a new record in the isostructural compounds.[18] We, thus, naturally conducted a systematic As doping study on Mo_5Si_3, which led to the discovery of superconductivity in $Mo_5Si_{3-x}As_x$.

Mo_5Si_3 crystallizes in a tetragonal W_5Si_3-type structure (space group *I*4/*mcm*), as illustrated in Figure 1a. Notice that there are two kinds of Si atoms taking different Wyckoff positions: Si1 at the 4*a* sites, and Si2 at the 8*h* sites. In this study, we show that arsenic can be doped into Mo_5Si_3. Interestingly, As atoms selectively takes the Si2 (8*h*) sites. Furthermore, superconductivity was observed in $Mo_5Si_{3-x}As_x$ ($x \geq 0.5$), with T_c increases from 4.4 K in $Mo_5Si_{2.5}As_{0.5}$ to 7.7 K in Mo_5Si_2As. The data for Mo_5Si_2As are shown in the main text, while additional information about $Mo_5Si_{3-x}As_x$ ($x \neq 1.0$) is shown in Figures S2−S4.

Figure 1c demonstrates the powder X-ray diffraction (XRD) pattern of Mo_5Si_2As. For Mo_5Si_2As, there are at least two configurations (configs.) in which As atoms take different sites (Figure 1b). In config. 1, As atoms randomly take the Si2 (8*h*) sites. While in config. 2, As atoms take all the Si1 (4*a*) sites. However, the observed XRD pattern can *only* be refined with config. 1. In particular, any occupation of As at the Si1 (4*a*) sites will cause a significant enhancement of the (200) peak, which prevents the refinement from convergence. (See Figure S5.) A brief list of the refined crystallographic parameters is shown in Table 1. More details about the refinement results can be found in Table S1. According to the refinement, there is about 10.3 wt % of Mo_3Si impurity in the sample. The refined composition is $Mo_{5.00(1)}Si_{1.97(3)}As_{1.05(8)}$, which is close to that determined by energy-dispersive X-ray spectroscopy. (For the sample morphology and elemental mapping, see Figure S6.)

The site-selective doping of As is further backed by the first-principles calculations. As shown in Figure 1b, the enthalpy (H) for config. 1 is lower compared with config. 2, which means As doping at the Si2 (8*h*) sites is more favorable in energy. The above conclusion is based on zero temperature calculations, but it is also true for finite temperatures. This is because the free energy $G = H - TS$, and the entropy S for config. 1 is larger. (Notice the Boltzmann relation $S = k_B \ln \Omega$, where k_B is the Boltzmann constant, and Ω is the number of microstates)

Figure 2a shows the temperature dependence of resistivity (ρ) of Mo_5Si_2As. The monotonous decrease of ρ upon cooling indicates a metallic nature. Superconducting transition is observed below 7.7(1) K (T_c^{onset}), with zero resistivity achieved at 7.4(1) K (T_c^{zero}). Figure 2b emphasizes the region of the

Received: May 12, 2022
Published: June 28, 2022

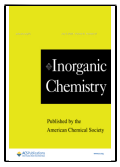

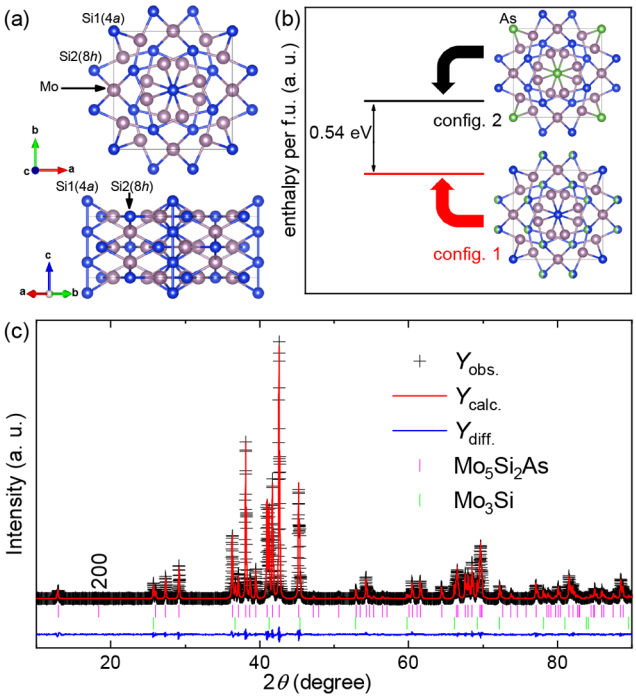

Figure 1. (a) Crystal structure of Mo_5Si_3. (b) Two possible configurations of Mo_5Si_2As and the corresponding enthalpies from DFT calculations. (c) Room-temperature XRD pattern of Mo_5Si_2As and its Rietveld refinement. The vertical bars indicate the Bragg positions for Mo_5Si_2As and the Mo_3Si impurity. The relevant (200) peak of Mo_5Si_2As is marked.

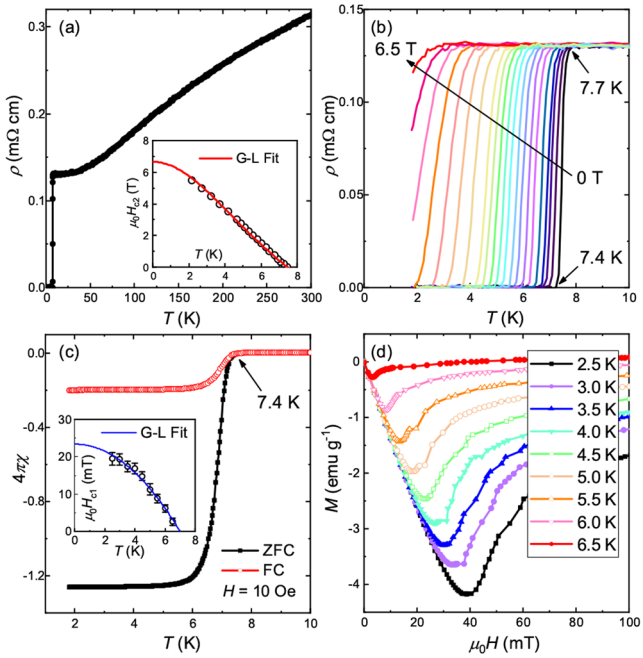

Figure 2. (a) Temperature dependence of resistivity (ρ) of Mo_5Si_2As under zero magnetic field. Inset shows the temperature dependence of upper critical field. (b) Zoom-in of the superconducting transition on $\rho(T)$ under magnetic fields from 0 to 6.5 T. (c) DC magnetic susceptibility of Mo_5Si_2As under 10 Oe. Inset shows the temperature dependence of lower critical field. (d) Isothermal magnetization at different temperatures.

superconducting transition. Upon the application of the magnetic field, the transition is gradually suppressed. The temperature dependence of upper critical field ($\mu_0H_{c2}(T)$) can thus be determined, which is shown in the inset of Figure 2a. A Ginzburg−Landau (G−L) fit gives $\mu_0H_{c2}(0) = 6.65(4)$ T.

DC magnetic susceptibility ($4\pi\chi$) of Mo_5Si_2As from 1.8 to 10.0 K under 10 Oe is demonstrated in Figure 2c. Bulk superconductivity is confirmed in $4\pi\chi(T)$ curves, with large diamagnetic signals observed below 7.4 K. The value of T_c determined from $4\pi\chi(T)$ agrees very well with that from $\rho(T)$. We also measured the isothermal magnetization curves for Mo_5Si_2As. The results are shown in Figure 2(d). The lower critical fields ($\mu_0H_{c1}(T)$) are determined from the deviation of the curves from initial Meissner states. As shown in the inset of Figure 2(c), $\mu_0H_{c1}(T)$ can be fitted with the G−L relation: $\mu_0H_{c1}(T) = \mu_0H_{c1}(0)[1 - (T/T_c)^2]$, giving $\mu_0H_{c1}(0) = 22.4(5)$ mT.

A series of superconducting parameters can be determined using $\mu_0H_{c2}(0)$ and $\mu_0H_{c1}(0)$. The values of these parameters are listed in Table 2. The definitions and calculation details for them can be found in Supporting Information. Notice $\kappa_{GL} \gg 1/\sqrt{2}$, suggesting type-II superconductivity in Mo_5Si_2As.

Table 2. Superconducting and Thermodynamic Parameters of Mo_5Si_2As

parameter (unit)	value
T_c^{onset} (K)	7.7(1)
T_c^{zero} (K)	7.4(1)
$\mu_0H_{c1}(0)$ (mT)	22.4(5)
$\mu_0H_{c2}(0)$ (T)	6.65(4)
$\mu_0H_c(0)$ (T)	0.22(0)
ξ_{GL} (nm)	7.03(2)
λ_{GL} (nm)	159.5(4)
κ_{GL}	22.7(1)
γ (mJ mol^{-1} K^{-2})	34.74(8)
β (mJ mol^{-1} K^{-4})	0.273(1)
Θ_D (K)	385(2)
λ_{ep}	0.66(1)
$\Delta C_e/\gamma T_c$	1.46(2)

The specific heat (C_p) of Mo_5Si_2As was measured to investigate the superconducting, as well as the thermodynamic

Table 1. Crystallographic Parameters of Mo_5Si_2As from Rietveld Refinement of XRD (R_p = 1.03%, R_{wp} = 1.49%)

atom (site)	x	y	z	U_{eq} (0.01 Å^2)	occupancy
Mo1 (4b)	0	0.5	0.25	0.137(27)	0.987(2)
Mo2 (16k)	0.07652(4)	0.22196(5)	0	0.392(17)	1.0
Si1 (4a)	0	0	0.25	0.84(15)	1.0
Si2/As (8h)	0.16592(8)	0.66592(8)	0	1.36(6)	0.474(4)/0.526

https://doi.org/10.1021/acs.inorgchem.2c01647
Inorg. Chem. 2022, 61, 10267−10271

properties. The results are shown in Figure 3(a). Notice the data have been corrected to exclude the influence of Mo_3Si impurity. Thermodynamic parameters for Mo_3Si were adopted from the literature.[19] Under zero magnetic field, C_p for Mo_5Si_2As clearly shows an anomaly at ~7.0 K, validating the bulk superconductivity. When a field of 8 T was applied, superconductivity was completely suppressed. The data under 8 T can be well fitted with the Debye model: $C_p(T) = \gamma T + \beta T^3$, giving $\gamma = 34.74(8)$ mJ mol^{-1} K^{-2}, and $\beta = 0.273(1)$ mJ mol^{-1} K^{-4}. The Debye temperature (Θ_D) is thus determined by $\Theta_D = (12\pi^4 NR/5\beta)^{1/3}$ to be 385(2) K. (N is the number of atoms in a formula unit (f.u.), and R is the ideal gas constant.) The electronic contribution of specific heat (C_e) is extracted by $C_e = C_p|_{\mu_0 H=0} - C_p|_{\mu_0 H=8T} + \gamma$, which is shown in Figure 3b. C_e at the superconducting state can be well fitted with the so-called α-model.[20] The normalized C_e change $\Delta C_e/\gamma T_c = 1.46(2)$, which is close to the BCS weak-coupling ratio (1.43). The electron−phonon coupling strength (λ_{ep}) can be estimated by using the inverted McMillan formula:[21]

$$\lambda_{ep} = \frac{1.04 + \mu^* \ln(\Theta_D/1.45T_c)}{(1 - 0.62\mu^*)\ln(\Theta_D/1.45T_c) - 1.04} \quad (1)$$

By setting the Coulomb screening parameter $\mu^* = 0.13$, a typical value for intermetallics, we get $\lambda_{ep} = 0.66(1)$. These results suggest a weak to moderate coupling in Mo_5Si_2As.

For comparison, we also measured the temperature dependence of C_p of Mo_5Si_3, which is shown in Figure 3a. γ and Θ_D for Mo_5Si_3 are estimated to be 19.80 mJ mol^{-1} K^{-2} and 659 K, respectively. These values are comparable with previous report on Mo_5Si_3 single crystals.[22] Notice that γ in Mo_5Si_2As is significantly larger than the undoped Mo_5Si_3, and the large decrease of Θ_D suggests substantial softening of the lattice. To take more insight into this, the density of states (DOS) was calculated for Mo_5Si_3 and Mo_5Si_2As. The results are shown in Figure 3c. One may notice the similar shapes of the DOS curves, which means that the bands can be considered rigid in our case. (For the band structures, see Figure S7) Arsenic doping shifts the Fermi level (E_F) to higher energy, causing a significant enhancement of DOS at E_F ($N(E_F)$). This is as expected, since As hosts one more valence electron compared with Si. $N(E_F)$ for Mo_5Si_3 is 4.13 eV^{-1} f.u.$^{-1}$, while $N(E_F)$ for Mo_5Si_2As is 7.37 eV^{-1} f.u.$^{-1}$. The enhancement of $N(E_F)$ led to the increase of γ. We can theoretically estimate the value of γ for Mo_5Si_2As by

$$\gamma = \frac{1}{3}N(E_F)\pi^2 k_B^2(1 + \lambda_{ep}) \quad (2)$$

to be ~29.02 mJ mol^{-1} K^{-2}, which agrees well with the experimental value. According to McMillan's formalism, $\lambda_{ep} = [N(E_F)\langle I^2\rangle]/[M\langle\omega^2\rangle]$, where M is the atomic mass, $\langle I^2\rangle$ and $\langle\omega^2\rangle$ stand for averages of the squared electronic matrix elements on the Fermi surface, and of the squared phonon frequencies, respectively.[21] The emergence of superconductivity in $Mo_5Si_{3-x}As_x$ should be due to the enhancement of $N(E_F)$, and possibly the softening of lattice (as evidenced by the large decrease of Θ_D).

Lastly, we would like to point out that a T_c of 7.7 K is fairly high in W_5Si_3-type superconductors. A comparison of T_c between Mo_5Si_2As and previously reported W_5Si_3-type superconductors is illustrated in Figure 4.[18,23−30] Notice that maximal T_c occurs when the average number of valence electrons per atom (e/a) ~ 4.6 or 5.4. Here, the second peak (at e/a ~ 5.4) is just a tentative guide, and is less reliable as there are only a few examples with $e/a > 5$. The phenomenon that T_c peaks at certain e/a values, known as the Matthias rule, has also been observed in other intermetallics.[31] Currently, the region of $e/a > 5.5$ remains unexplored, so more superconductors may be discovered if more electrons can be introduced into this structural family.

In summary, we report the discovery of superconductivity in $Mo_5Si_{3-x}As_x$ ($0.5 \le x \le 1.25$), in which a maximal T_c of 7.7 K

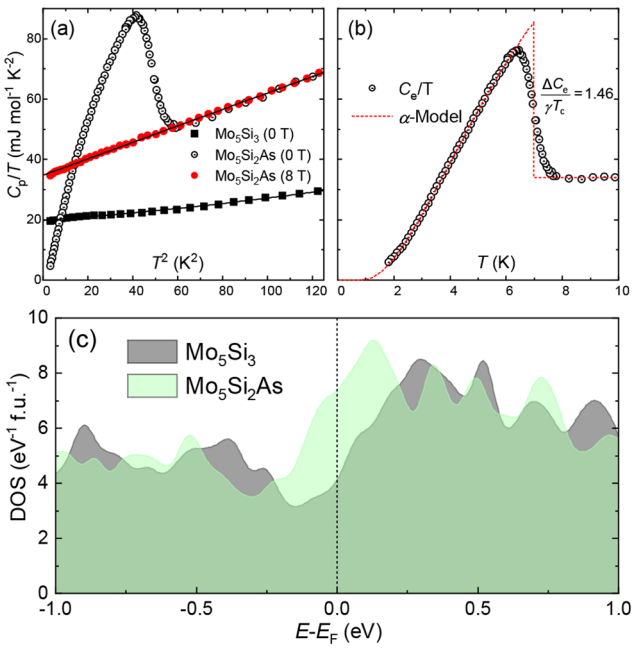

Figure 3. (a) Temperature dependence of specific heat (C_p) of Mo_5Si_2As under zero magnetic field, and under a field of 8 T. The C_p data for Mo_5Si_3 are also plotted for comparison. Solid lines are fittings with Debye model. (b) Temperature dependence of the electronic contribution of C_p under zero magnetic field. Parts a and b share the same y-axis range. (c) Calculated DOS for Mo_5Si_3 and Mo_5Si_2As near the Fermi level.

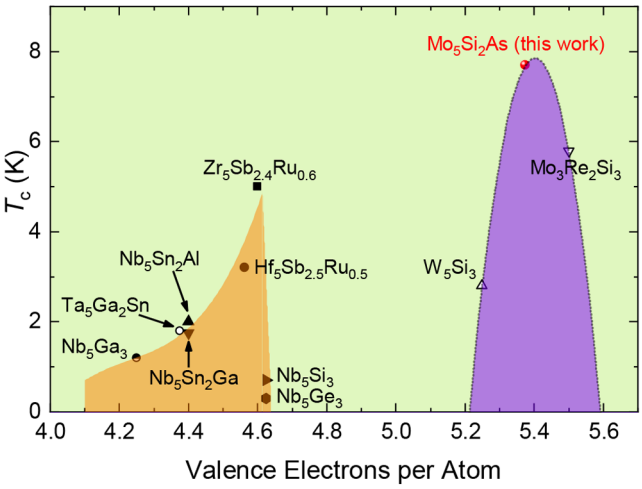

Figure 4. Evolution of T_c in W_5Si_3-type superconductors upon the valence electron per atom (e/a). Note that the peak at e/a ~ 5.4 is just a tentative guide.

https://doi.org/10.1021/acs.inorgchem.2c01647
Inorg. Chem. 2022, 61, 10267−10271

is observed in Mo_5Si_2As. Arsenic doping in Mo_5Si_3 is found to be site-selective. According to specific heat measurements and first-principles calculations, the emergence of superconductivity is related to the shift of Fermi level. Our method of As doping should be generally applicable to other silicides, in which more superconductors can be expected.

■ ASSOCIATED CONTENT

Supporting Information

The Supporting Information is available free of charge at https://pubs.acs.org/doi/10.1021/acs.inorgchem.2c01647.

Experimental and calculation details, evolution of lattice parameters and superconducting properties of $Mo_5Si_{3-x}As_x$ ($0 \leq x \leq 1.25$), discussion on the site-selective doping in Mo_5Si_2As, detailed XRD refinement results, SEM images, elemental mapping, and band structure for Mo_5Si_2As (PDF)

■ AUTHOR INFORMATION

Corresponding Authors

Bin-Bin Ruan − *Institute of Physics and Beijing National Laboratory for Condensed Matter Physics, Chinese Academy of Sciences, Beijing 100190, China;* orcid.org/0000-0003-4642-7782; Email: bbruan@mail.ustc.edu.cn

Zhi-An Ren − *Institute of Physics and Beijing National Laboratory for Condensed Matter Physics, Chinese Academy of Sciences, Beijing 100190, China; School of Physical Sciences, University of Chinese Academy of Sciences, Beijing 100049, China;* orcid.org/0000-0003-4308-7372; Email: renzhian@iphy.ac.cn

Authors

Jun-Nan Sun − *Information Materials and Intelligent Sensing Laboratory of Anhui Province, Institutes of Physical Science and Information Technology, Anhui University, Hefei 230601, China; Key Laboratory of Structure and Functional Regulation of Hybrid Materials (Anhui University), Ministry of Education, Hefei 230601, China*

Meng-Hu Zhou − *Institute of Physics and Beijing National Laboratory for Condensed Matter Physics, Chinese Academy of Sciences, Beijing 100190, China*

Qing-Song Yang − *Institute of Physics and Beijing National Laboratory for Condensed Matter Physics, Chinese Academy of Sciences, Beijing 100190, China; School of Physical Sciences, University of Chinese Academy of Sciences, Beijing 100049, China*

Ya-Dong Gu − *Institute of Physics and Beijing National Laboratory for Condensed Matter Physics, Chinese Academy of Sciences, Beijing 100190, China; School of Physical Sciences, University of Chinese Academy of Sciences, Beijing 100049, China*

Gen-Fu Chen − *Institute of Physics and Beijing National Laboratory for Condensed Matter Physics, Chinese Academy of Sciences, Beijing 100190, China; School of Physical Sciences, University of Chinese Academy of Sciences, Beijing 100049, China; Songshan Lake Materials Laboratory, Dongguan, Guangdong 523808, China*

Lei Shan − *Information Materials and Intelligent Sensing Laboratory of Anhui Province, Institutes of Physical Science and Information Technology, Anhui University, Hefei 230601, China; Key Laboratory of Structure and Functional Regulation of Hybrid Materials (Anhui University), Ministry of Education, Hefei 230601, China*

Complete contact information is available at: https://pubs.acs.org/10.1021/acs.inorgchem.2c01647

Notes

The authors declare no competing financial interest.

■ ACKNOWLEDGMENTS

This work was supported by the National Key Research and Development of China (Grant Nos. 2018YFA0704200, 2021YFA1401800, 2018YFA0305602, and 2017YFA0302904), the National Natural Science Foundation of China (Grant Nos. 12074414, 12074002, and 11774402), and the Strategic Priority Research Program of Chinese Academy of Sciences (Grant No. XDB25000000).

■ REFERENCES

(1) Trumbore, F. A. Solid solubilities of impurity elements in germanium and silicon. *Bell System Technical Journal* **1960**, *39*, 205−233.

(2) Masetti, G.; Severi, M.; Solmi, S. Modeling of carrier mobility against carrier concentration in arsenic-, phosphorus-, and boron-doped silicon. *IEEE Trans. Electron Devices* **1983**, *30*, 764−769.

(3) Ramamoorthy, M.; Pantelides, S. T. Complex dynamical phenomena in heavily arsenic doped silicon. *Phys. Rev. Lett.* **1996**, *76*, 4753.

(4) Boller, H.; Wolfsgruber, H.; Nowotny, H. Röntgenographische Untersuchungen in den Systemen Chrom-Silicium (Germanium)-Arsen. *Monatsh. Chem.* **1967**, *98*, 2356−2361.

(5) Ellner, M.; El-Boragy, M. Über die eisenhaltigen vertreter des strukturtyps Pd_5Sb_2. *J. Alloys Compd.* **1992**, *184*, 131−138.

(6) Wang, C.; Hughbanks, T. Main group element size and substitution effects on the structural dimensionality of zirconium tellurides of the ZrSiS type. *Inorg. Chem.* **1995**, *34*, 5524−5529.

(7) Grosvenor, A. P.; Cavell, R. G.; Mar, A.; Blyth, R. I. Analysis of the electronic structure of $Hf(Si_{0.5}As_{0.5})As$ by X-ray photoelectron and photoemission spectroscopy. *J. Solid State Chem.* **2007**, *180*, 2670−2681.

(8) Gaultois, M. W.; Grosvenor, A. P.; Blanchard, P. E.; Mar, A. Ternary arsenides $Zr(Si_xAs_{1-x})As$ with $PbCl_2$-type ($0 \leq x \leq 0.4$) and PbFCl-type (x = 0.6) structures. *J. Alloys Compd.* **2010**, *492*, 19−25.

(9) Rundqvist, S.; Sillén, L.; Timm, D.; Motzfeldt, K.; Theander, O.; Flood, H. Phosphides of the B31 (MnP) structure type. *Acta Chem. Scand.* **1962**, *16*, 287−292.

(10) Adachi, H.; Imoto, S. Energy Band Structure of Uranium Compounds with NaCl Type Structure. *J. Nucl. Sci. Technol.* **1969**, *6*, 371−379.

(11) Lomnytska, Y. F.; Oryshchyn, S.; Kuz'ma, Y. B.; Guerin, R. Crystal Structure of $Nb_5Si_{3-x}P_{0.5+x}$ (x = 0−0.5). *Inorg. Mater.* **2005**, *41*, 1067−1072.

(12) Svitlyk, V.; Miller, G. J.; Mozharivskyj, Y. $Gd_5Si_{4-x}P_x$: Targeted Structural Changes through Increase in Valence Electron Count. *J. Am. Chem. Soc.* **2009**, *131*, 2367−2374.

(13) Kirschen, M.; Vincent, H.; Perrier, C.; Chaudouet, P.; Chenevier, B.; Madar, R. Synthesis and crystal structure of rhodium and iridium new phospho-silicides. *Mater. Res. Bull.* **1995**, *30*, 507−513.

(14) Perrier, C.; Kreisel, J.; Vincent, H.; Chaix-Pluchery, O.; Madar, R. Synthesis, crystal structure, physical properties and Raman spectroscopy of transition metal phospho-silicides MSi_xP_y (M = Fe, Co, Ru, Rh, Pd, Os, Ir, Pt). *J. Alloys Compd.* **1997**, *262*−*263*, 71−77.

(15) Mu, Q.-G.; Ruan, B.-B.; Zhao, K.; Pan, B.-J.; Liu, T.; Shan, L.; Chen, G.-F.; Ren, Z.-A. Superconductivity at 10.4 K in a novel quasi-one-dimensional ternary molybdenum pnictide $K_2Mo_3As_3$. *Sci. Bull.* **2018**, *63*, 952−956.

(16) Zhao, K.; Mu, Q.-G.; Ruan, B.-B.; Zhou, M.-H.; Yang, Q.-S.; Liu, T.; Pan, B.-J.; Zhang, S.; Chen, G.-F.; Ren, Z.-A. A New Quasi-One-Dimensional Ternary Molybdenum Pnictide $Rb_2Mo_3As_3$ with Superconducting Transition at 10.5 K. *Chin. Phys. Lett.* **2020**, *37*, 097401.
(17) Zhao, K.; Mu, Q.-G.; Ruan, B.-B.; Liu, T.; Pan, B.-J.; Zhou, M.-H.; Zhang, S.; Chen, G.-F.; Ren, Z.-A. Synthesis and superconductivity of a novel quasi-one-dimensional ternary molybdenum pnictide $Cs_2Mo_3As_3$. *APL Mater.* **2020**, *8*, 031103.
(18) Wu, J.; Hua, C.; Liu, B.; Cui, Y.; Zhu, Q.; Xiao, G.; Wu, S.; Cao, G.; Lu, Y.; Ren, Z. Doping-induced superconductivity in the topological semimetal Mo_5Si_3. *Chem. Mater.* **2020**, *32*, 8930−8937.
(19) Jorda, J. L. In *Mo based alloys and compounds (continued): Datasheet from Landolt-Börnstein - Group III Condensed Matter*; "Ac-Na" in SpringerMaterials 21A; Flükiger, R., Klose, W., Eds.; Springer-Verlag Berlin Heidelberg: 1990.
(20) Padamsee, H.; Neighbor, J.; Shiffman, C. Quasiparticle phenomenology for thermodynamics of strong-coupling superconductors. *J. Low Temp. Phys.* **1973**, *12*, 387−411.
(21) McMillan, W. L. Transition Temperature of Strong-Coupled Superconductors. *Phys. Rev.* **1968**, *167*, 331.
(22) Ito, K.; Hayashi, T.; Nakamura, H. Electrical and thermal properties of single crystalline Mo_5X_3 (X= Si, B, C) and related transition metal 5−3 silicides. *Intermetallics* **2004**, *12*, 443−450.
(23) Jorda, J.; Flükiger, R.; Muller, J. On the formation and stability of the A15 phase in the niobium-gallium system. *J. Less-Common Met.* **1977**, *55*, 249−264.
(24) Shishido, T.; Ukei, K.; Toyota, N.; Sasaki, T.; Watanabe, Y.; Motai, K.; Fukuda, T.; Takeya, H.; Takei, H. Flux growth of a new ternary superconducting crystal Nb_5Sn_2Ga. *J. Cryst. Growth* **1989**, *96*, 1−6.
(25) Shishido, T.; Ye, J.; Toyota, N.; Ukei, K.; Sasaki, T.; Horiuchi, H.; Fukuda, T. Growth and superconductivity of a new ternary intermetallic compound, Ta_5Ga_2Sn. *Jpn. J. Appl. Phys., Part 1* **1989**, *28*, 1519.
(26) Claeson, T.; Ivarsson, J.; Rasmussen, S. Superconductivity of Nb_5Ge_3. *J. Appl. Phys.* **1977**, *48*, 3998.
(27) Xie, W.; Luo, H.; Phelan, B.; Cava, R. $Zr_5Sb_{3-x}Ru_x$, a new superconductor in the W_5Si_3 structure type. *J. Mater. Chem. C* **2015**, *3*, 8235−8240.
(28) Xie, W.; Luo, H.; Seibel, E. M.; Nielsen, M. B.; Cava, R. J. Superconductivity in $Hf_5Sb_{3-x}Ru_x$: Are Ru and Sb a Critical Charge-Transfer Pair for Superconductivity? *Chem. Mater.* **2015**, *27*, 4511−4514.
(29) Wu, J.; Liu, B.; Cui, Y.; Wang, H.; Wang, Z.; Ren, Z.; Cao, G. Type-II superconductivity in W_5Si_3-type Nb_5Sn_2Al. *Supercond. Sci. Technol.* **2019**, *32*, 045010.
(30) Kawashima, K.; Muranaka, T.; Kousaka, Y.; Akutagawa, S.; Akimitsu, J. Superconductivity in transition metal-silicide W_5Si_3. *J. Phys.: Conf. Ser.* **2009**, *150*, 052106.
(31) Matthias, B. T. Empirical Relation between Superconductivity and the Number of Valence Electrons per Atom. *Phys. Rev.* **1955**, *97*, 74−76.

https://doi.org/10.1021/acs.inorgchem.2c01647
Inorg. Chem. 2022, 61, 10267−10271